

## Microstructure and CTOD (crack tip opening displacement) of Deposit Weld Metal in 30 mm Thick Plate

Hae-Woo Lee<sup>†</sup>, Hyok-Ju Kim, Jeong-Ung Park\*, Chang-Yong Kang\*\* and Jang-Hyun Sung\*\*\*

Welding research team, Samsung heavy industries, Gyungnam 656-710

\*Department of Civil engineering, Chosun university, Gwangju 501-759

\*\*Div. of Mat. Sci. and engineering, Pukyong national university, Busan 608-031

\*\*\*Department of metallurgical engineering, Dong-A university, Busan 604-714

(2004년 5월 17일 받음, 2004년 9월 4일 최종수정본 받음)

**Abstract** The microstructure and crack tip opening displacement (CTOD) of deposit weld metal were investigated for a 30 mm- thick plate welded with flux cored arc welding (FCAW) and submerged arc welding (SAW) processes. The CTOD test was carried out both as welded condition and as stress-relieved specimen by local compression. The crack growth rates in FCAW were faster than those in a SAW, and the acicular ferrite content by the SAW process was increased relatively more than that by the FCAW process. The fatigue crack growth rate in a welded specimen was faster than that in locally compressed specimen. The CTOD value of locally compressed specimens was lower than that of as welded specimen. Furthermore, the CTOD value tested with the SAW process was higher than that tested with the FCAW process.

**Key words** CTOD, SAW, FCAW, heat input, pre-cracking, three-point bending, acicular ferrite.

### 1. Introduction

As welded structures become bigger, thick-plate welding becomes more important. Thick-plate weldments have higher cooling rates and greater residual stresses than thin-plate weldments. As-deposited weld metals and weld metals reheated to various temperatures by the subsequent beads are present in a multi-layer thick plate weldments.

The weldments are the weakest area because heating and cooling creates inconsistent microstructure. Safety is very important in this type of weld fabrication. Toughness, especially, plays an important role in weldments with respect to the quality and reliability of a welded construction.<sup>1-3)</sup> The crack tip opening displacement (CTOD) tests were performed to determine the fracture toughness of 30 mm-thick deposit weld metals.

The CTOD test was carried out on both as welded condition specimens and as stress-relieved specimens by local compression. Local compression is a technique whereby mechanical stress is relieved at the weldment by inserting a hardened steel platen into the local region in front of the machined notch before fatigue pre-cracking. For this "local compression" technique to be effective in

the sufficient relief of residual stresses to obtain uniform fatigue cracks, a total plastic strain applied across 1% of the thickness of the specimen was found to be the minimum practical.<sup>2)</sup>

Until now, few investigations on the CTOD characteristics in deposit weld metals according to heat input have been conducted.

In this study, therefore, CTOD characteristics, hardness, and microstructure were studied according to FCAW and SAW processes.

### 2. Experimental Procedures

#### 2.1 Test panel/Welding

The size of the test panel was 1500 mm long × 400 mm wide × 30 mm thick as shown in Fig. 1. The panel was fabricated from API 2H Gr.50 higher-strength steel for offshore structure. The specimen sections were welded under the following conditions as shown in Fig. 2.

1) heat input of 20 kJ/cm by the FCAW process.

2) heat input of 33 kJ/cm by the SAW 1 pole process.

The FCAW test panel was welded following the DW-100(AWS A5.20 E71T) specification, while the SAW test panel was welded following the S-777MX × H-14(AWS F7A(P)-2 × EH14) specification. Welding parameters are

<sup>†</sup>E-Mail : hw6308@hanmail.net

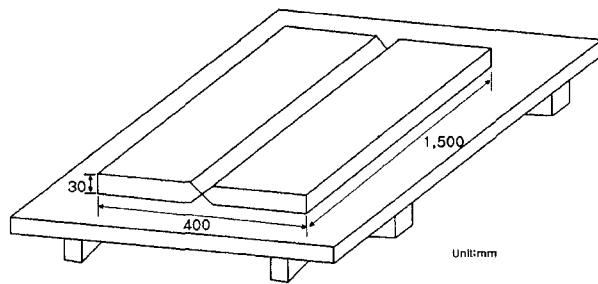


Fig. 1. Schematic diagram of weld panel.

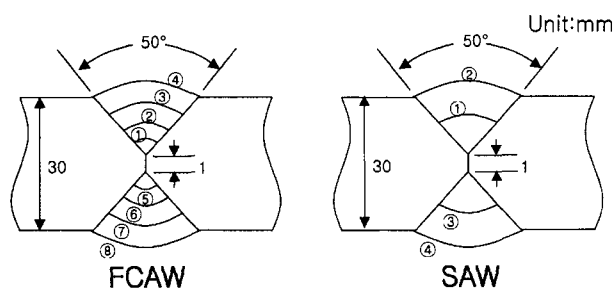


Fig. 2. Schematic diagram of deposited weld panel.

shown in Table 1.

## 2.2 Chemical composition/ Microstructure/ Hardness distribution

A spectro-analyzer (BAIRD, Specrovac-2000) was used to determine the chemical composition of the deposited weld metals. The mean values of the chemical composition are provided in Table 2.

The specimens were prepared by polishing with a one micron alumina abrasive, followed by etching for 10-15 s in a solution of 2% Nital. A standard point counting technique was used to determine the volume fraction of acicular ferrite at a magnification of  $500\times$ . A micro-

structural constituent was classified based on the guideline suggested by Pargeter and Dolby.<sup>4)</sup> Hardness was measured using the macro Vickers hardness test, with a load of 10 kg and 10 s of loading time. Measurements were made on the transverse section at 10 mm from the top surface.

## 2.3 CTOD Test

### 2.3.1 Morphology of specimen

The CTOD test specimens were made from as deposited weld metal along the welding line (NP specimen, BS7448 part 2).

The test was carried out on two kinds of samples: One was a sample under the as-welded condition, and the other was a stress-relieved sample obtained by local compression. Local compression is a technique whereby mechanical stress is relieved at the weldment using a hardened steel platen into the local region in front of the machined notch before the fatigue pre-cracking. The morphology of the specimen is shown in Fig. 3.

### 2.3.2 Fatigue pre-cracking test

Test equipment was a  $\pm 25$  ton capacity, uniaxial tension fatigue test machine. Testing was performed at the load control condition at a stress ratio = 0.05 with sine wave and frequency of 3 Hz at room temperature.

Fatigue pre-cracking force was solved from equation,<sup>1)</sup> and the crack length was made long enough, considering the strain-hardening in the machined notch.<sup>5,6)</sup>

$$K_f = \frac{Y P_f}{B W^{1/2}} < 0.63 \sigma_Y B W^{1/2} \quad (1)$$

$K_f$  = Fatigue stress intensity factor

$Y$  = Stress intensity coefficient

$P_f$  = Fatigue pre-cracking force

$B$  = Test piece thickness

Table 1. Welding parameters

	Filler metals		Current (A)	Voltage (V)	Welding speed (cm/min.)	Heat input (kJ.cm)
	AWS spec.	Diameters (mm)				
FCAW	A5.20 E71T-1	1.4	300	34	30	20
SAW	F7A(P)-2EH14	4.8	650	34	40	33

Table 2. Chemical composition of deposited weld metal.

	C (wt-%)	Si (wt-%)	Mn (wt-%)	P (wt-%)	S (wt-%)	Al (wt-%)	Cu (wt-%)	Ni (wt-%)	O (wt-%)
FCAW	0.08	0.44	1.24	0.015	0.016	0.03	0.01	0.06	262
SAW	0.12	0.38	1.43	0.018	0.016	0.03	0.13	0.07	295

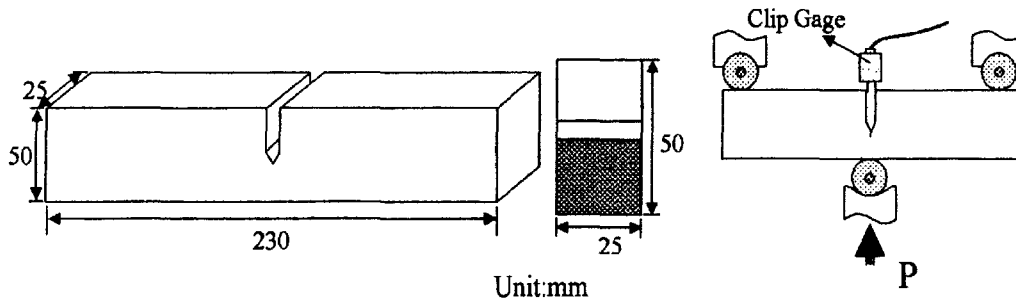


Fig. 3. Schematic diagram of CTOD test specimen and equipment.

W = Test piece width  
 $\sigma_Y = 0.2\%$  proof stress at temperature of interest

$V_p$  = Plastic component of clip gage displacement  
 z = Distance of clip gage location from test piece surface

2.3.3 Three-point bending test

The three-point bending test was carried out at  $-10^\circ\text{C}$  chamber with the specimens placed in methyl alcohol for 30 seconds per 1 mm-thickness.

The test carried out at the condition in which the increasing rate of stress intensity factor during the initial elastic deformation was controlled within the range of  $15 \text{ Nmm}^{-3/2}$  to  $80 \text{ Nmm}^{-3/2}$  seconds (Poisson's ratio of 0.3).

The displacement was measured by using a COD gage(clip gage), whose travel length is 4 mm, and the load-displacement curve was derived by using the (SERIES IX) program.<sup>5,6)</sup>

$$\frac{108 \times B^{1/2}}{E} \text{ mm/s} < \text{Loading rate} < \frac{575 \times B^{1/2}}{E} \text{ mm/s} \quad (2)$$

B = Test piece thickness  
 E = Young's modulus

2.3.4 Crack measurement after fracture

After completion of the test, the fracture surface was examined on the basis of BS 5762; the fatigue crack length was respectively measured for 25%, 50%, 75% of the thickness of the specimen; and the maximum-minimum length of crack was measured by using a 20x magnifier.

2.3.5 Determination of CTOD

CTOD was measured in equation.<sup>3)</sup> It was compared and scrutinized with the standard CTOD (0.38 mm), the required value in offshore construction.<sup>5,6)</sup>

$$\delta = \frac{K^2(1 - \nu^2)}{2\sigma_Y E} + \frac{0.4(W - a)V_p}{0.4W + 0.6a + z} \quad (3)$$

K = Stress intensity factor  
 a = Effective crack length

3. Results and discussion

3.1 Macro/ Microstructure

The macrostructure of the weldments are shown in Fig. 4. Some significant differences can be noted between the heat affected zone that formed due to the welding pass and the heat affected zone located near the weld interface, these differences resulting in the most brittle section of the weld joints. Impact values improved in the reheated zone because the grain boundary ferrite and Widmanstatten side plate were transformed into pearlite and ferrite, and the grain size was refined.

Fig. 5A shows microstructure of the base metal, consisting of ferrite(white area), pearlite(dark area) and bainite (slightly gray area). The microstructure was affected by not

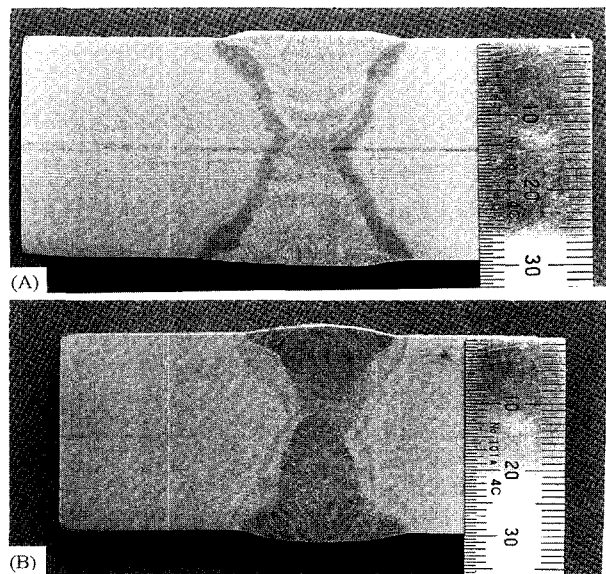
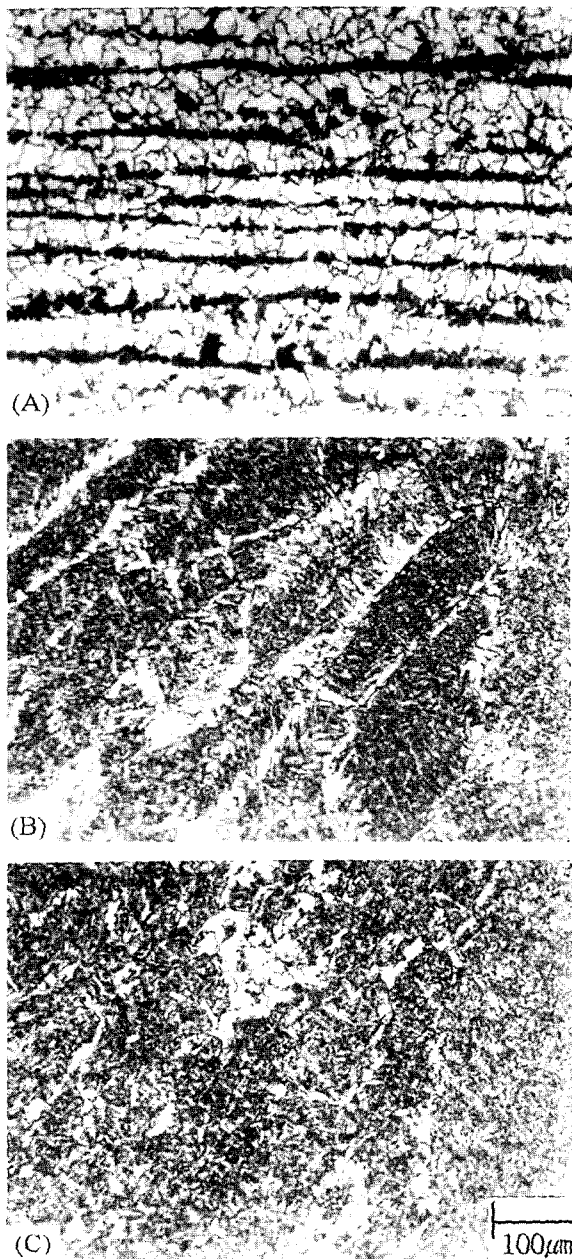


Fig. 4. Macrostructure of weld joints. (A): FCAW (B): SAW

only the heat input but also its chemical composition, welding process, cooling rate etc. The fine grain size results in excellent strength and toughness.<sup>7,8)</sup> Fig. 5B and C show an optical micrograph taken from the deposited weld metal area as a function of the welding process, revealing grain boundary ferrite, Widmanstatten side plate and acicular ferrite. To improve mechanical properties such as tensile and toughness, acicular ferrite has to form fully instead of forming grain boundary ferrite and Widmanstatten side plate.

The acicular ferrite content in the specimen welded with



**Fig. 5.** Microstructure of base metal and deposit weld metals. (A): Base metal (B): FCAW (C): SAW.

SAW process was transformed approximately 90%, while in the specimen welded with FCAW process was transformed 81%. In contrast, the primary ferrite such as grain boundary ferrite and Widmanstatten side plate increased in the specimen welded with the FCAW process as shown in Figs. 5B and 5C.

Bonnet and Charpentier<sup>9)</sup> reported the effect of titanium on acicular ferrite formation. They found that the additions of titanium above 0.0045 wt% in weld metal were produced due to a large volume fraction of acicular ferrite.

The effect of oxygen on the weld metal properties was reported. The properties such as toughness and weld metal plasticity were significantly affected by oxygen.<sup>10,11)</sup> The optimum oxygen content of a weld metal was in the range of 200–350 ppm, and the oxygen was mainly in the form of fine dispersed oxide inclusions of size less than 0.03 μm. Welds with a lowered oxygen content of 200 ppm also displayed the tendency to decrease in the plasticity because 1) the ferritic-pearlitic matrix of improved purity is

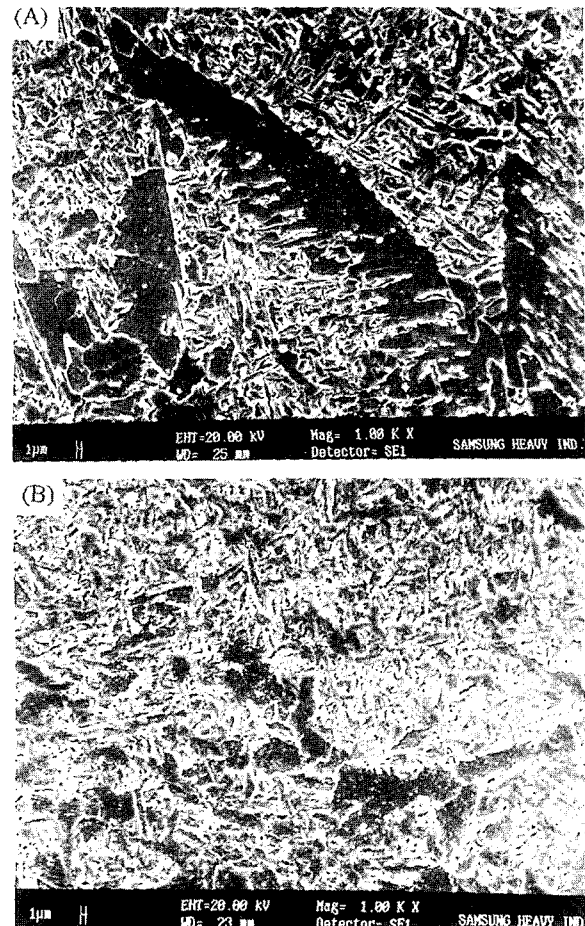


**Fig. 6.** SEM morphology of deposit weld metals. (A): FCAW (B): SAW.

likely to generate unbalanced structures on cooling and 2) the shapes of the sulfur and phosphor precipitations from the melt changes from globular to film-like form when there are no oxide inclusions. In a weld having more than 350 ppm of oxygen content, the oxygen inclusion precipitates partially along the grain boundaries. These inclusions block the dislocations and serve as crack nuclei when the metal is deformed.

### 3.2 Hardness distribution

Fig. 7 shows the hardness distribution 10 mm away from the weld surface with the FCAW and SAW processes. The relatively low heat input from the FCAW process produced a narrow HAZ of approximately 2 mm in width. In the specimen welded with the FCAW, the value of hardness (Hv) in the deposited weld metal was about Hv 10 higher than that in the specimen welded with the SAW. Especially, the value of hardness of the heat affected zone in the specimen welded with FCAW was about Hv 40 higher than that welded with SAW because the hardened structures such as martensite and bainite were easily transformed due to the rapid cooling rate.

### 3.3 Fatigue crack propagation

Fig. 8 shows the fatigue crack growth rates vs the stress intensity factor range for the as-welded specimens.

The crack growth rates in the flux-cored arc welding was faster than those in the submerged arc welding because the acicular ferrite contents in the specimen that underwent the SAW process were more transformed into acicular ferrite than those of that underwent the FCAW process. The cracks, therefore, easily propagated along the grain-boundary ferrite.

Chung, et al.<sup>12)</sup> have shown that the micromechanisms of fracture process are identified by observing the fracture in a single edge notched specimen through in-situ scanning electron microscopy (SEM). The observation of the in-situ fracture process for as-deposited top bead indicated that as strains were applied, microcracks were formed at the interfaces between the grain-boundary ferrite and the acicular ferrite under relatively low stress intensity factor. Then, the microcracks propagated easily along the proeutectoid ferrite phase, leading to a final fracture. It is noted that proeutectoid ferrite plays an important role in reducing the toughness of the weld metal.

The fatigue crack growth rate vs the stress intensity factor range for locally compressed specimens are plotted in Fig. 9. And also Table 3 shows the material constants,  $c$

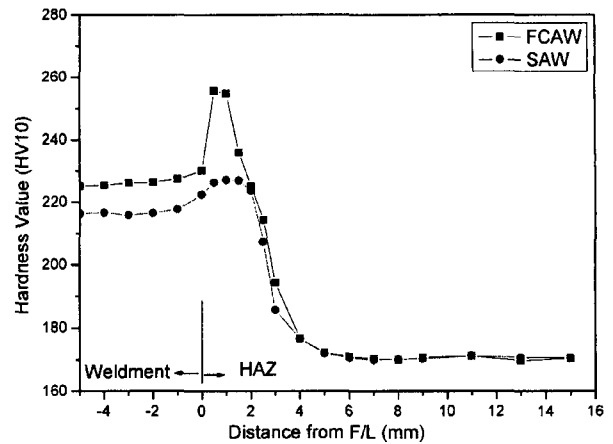


Fig. 7. Hardness distribution depending on welding process.

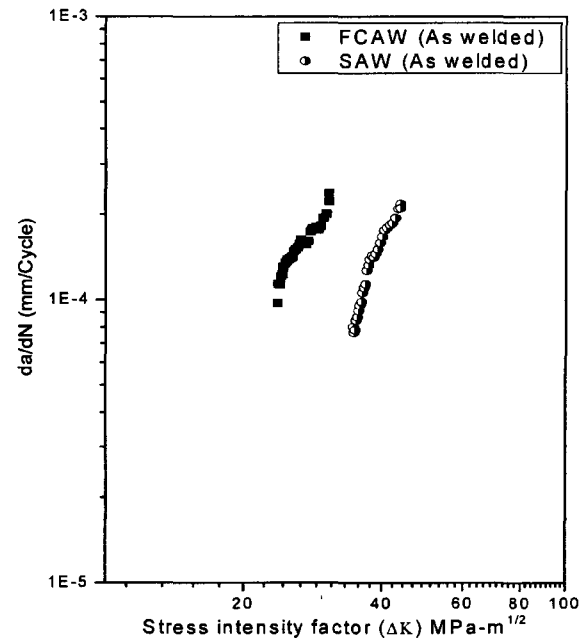


Fig. 8. Fatigue crack growth of as welded specimen.

and  $m$ , for Paris's equation.

The fatigue crack growth rate in the as welded specimens was faster than that of locally compressed specimens as shown in Figs. 8 and 9. The observed retardation in the crack growth rate in locally compressed specimens has been attributed to the redistribution of residual stress introduced by local compression.

The fatigue crack growth rate decreased as the fatigue crack increased, and these test results were in agreement with the results of Kapadia<sup>13)</sup> and Ohta.<sup>14)</sup>

### 3.4 Evaluation of CTOD

The mean CTOD value is shown in Table 4. The CTOD

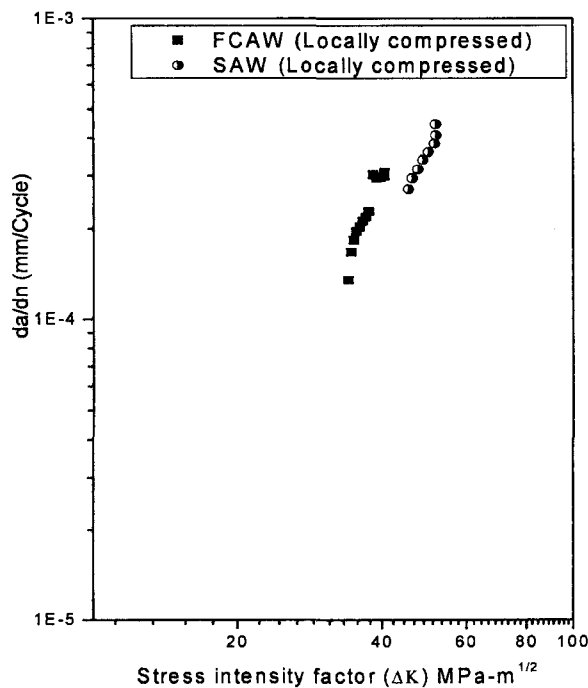


Fig. 9. Fatigue crack growth of locally compressed specimen.

values tested for the specimen that underwent the SAW process were higher than those that underwent the FCAW process.

It is noted that the acicular ferrite content of the specimen that underwent the SAW process was transformed relatively more than the specimen that underwent the FCAW process.

Toughness can be improved when the acicular ferrite forms fully instead of the grain boundary ferrite and Widmanstätten ferrite.

The table shows that the CTOD value of a locally compressed specimen is lower than that of an as-welded specimen

in all welding processes.

The microstructure is hardened due to plastic strains during local compression. An important consideration is the extent to which the plastic strains induced by local compression affects the fracture toughness.

Dawes<sup>15)</sup> have studied the effects of local compression by 1% of thickness on fracture toughness. He found that local compression appears to reduce the fracture toughness for the materials tested;- for example, for specimens tested at 100, the mean critical value of stress intensity factor  $K_c$  was 28% lower for locally compressed specimens than that of non-locally compressed specimens. In addition, the CTOD values between the test results and the results by Dawes<sup>15)</sup> were very similar.

#### 4. Conclusions

The crack tip opening displacement (CTOD) and microstructure were studied for 30 mm-thick plate welded with FCAW and SAW processes.

The results of this study are summarized as follows:

- 1) The mean CTOD value of the specimen welded with SAW process was higher than that welded with FCAW process and was increased with the amount of acicular ferrite.
- 2) The acicular ferrite content welded with SAW process was transformed relatively more than that welded with the FCAW process.
- 3) The mean CTOD value of a locally compressed specimen was lower than that of a as-welded specimen.
- 4) The fatigue crack growth rate of the flux-cored arc welding was faster than that of the submerged arc welding.

Table 3. Material constants ; C and m for Paris' equation.

	As welded specimen		Locally compressed specimen	
	FCAW	SAW	FCAW	SAW
m	3.60	3.72	2.25	3.13
log c	-20.7	-22.5	-16.6	-20.2

Table 4. Average CTOD values depending on welding process.

condition	FCAW				SAW			
	As welded		Locally compressed		As welded		Locally compressed	
CTOD (mm)	No. 1	0.15	No. 4	0.08	No. 7	0.43	No. 10	0.33
	No. 2	0.23	No. 5	0.20	No. 8	0.38	No. 11	0.35
	No. 3	0.32	No. 6	0.17	No. 9	0.36	No. 12	0.25
Mean	0.23		0.15		0.39		0.31	

## References

1. O. L. Towers and M. G. Dawes, *Journal of testing and evaluation*, **11**(1), 34 (1983).
2. M. G. Dawes, *Metal construction and British welding Journal*, **3**(2), 61 (1971).
3. H. W. Lee and S. W. Kang, *Welding Journal, American Welding Society*, **80**(6), 137 (2001).
4. R. J. Pargeter and R. E. Dolby, in *Proceedings of the American welding society, IIW Doc. IX-1377-85*, Miami, Fla., (1985).
5. BS 5762 : *Methods for crack opening displacement testing*, British standards institution, (1979).
6. BS 7448 : *Fracture mechanics toughness test part I and part II*, BSI, (1997).
7. S. Kou, *Welding Metallurgy*, John Wiley and Sons, New York, p. 326-333 (1987).
8. H. W. Lee, S. W. Kang and D. S. Um, *Welding Journal, American Welding Society*, **77**(12), 503 (1998).
9. C. Bonnet and F. P. Charpentier, in *Proceeding of the welding institute*, p. 8, Abington, U.K., (1996).
10. N. N. Potapov, *Welding Journal*, **72**(8), 367 (1993).
11. J. W. Hooijmans and G. D. Ouden, *Welding Journal*, **71**(10), 377 (1992).
12. H. H. Chung, C. M. Kim, H. S. Kim, W. S. Kim and S. H. Hong, *Korean welding journal*, **17**(2), 98 (1999).
13. B. M. Kapadia, *ASTM STP 648*, 244-260 (1978).
14. Akihito Ohta and Satoshi Nishijima, *The Society of materials science*, **1**, 157 (1985).
15. M. G. Dawes, Ph. D thesis, Council for national academic awards, London, England, p. 85 (1976).